DELAMINATION ANALYSIS OF COMPOSITES BY DISCRETE ELEMENT METHOD

S. Mohammadi, D.R.J. Owen and D. Peric

Department of Civil Engineering, University of Wales Swansea
Singleton Park, Swansea SA2 8PP, U.K.

Abstract. A combined finite/discrete element method is developed to model delamination behaviour in laminated composites. The failure surface for delamination is defined by a Chang-Springer criterion, and the interlaminar crack propagation is achieved by a standard discrete element contact/release algorithm. The performance of the method is assessed by solving test cases available from the literature.

1 INTRODUCTION

Although the major proportion of today's aircraft structures is still produced from lightweight aluminum alloys, there is an increasing trend towards usage of composite materials. One of the major problems that effects the design and performance of composite materials for structural applications is their vulnerability to transverse impact which may cause substantial internal damage of the component due to matrix cracking, fiber failure and delamination. There is, however, agreement that the most dominant causes of damage are matrix cracking coupled with complex mode delamination mechanisms [1, 2, 3].

In early simulations of delamination, a simple criterion based on the comparison of normal stress to a maximum cohesion value was used. Later, more complex models were developed for different types of laminates. More rational models were achieved by development of contact algorithms for modelling the interface behaviour of laminate composites containing multiple delaminations [4] in which the Chang-Springer model were widely adopted as the delamination initiation criterion [5].

It should be noted that in a real situation, delamination failure is always accompanied by inplane failures, including matrix and fiber fractures. The traditional elasticity and fracture mechanics methods are applicable in situations dealing with a low-fractured area. However in a highly fractured region, discontinuum based mechanics has been found to be more appropriate. The treatment of these classes of problems is naturally related to discrete element concepts, in which distinctly seperate material regions are considered which may be interacting with other discrete elements through a contact type interaction [6].

In this study, a combined finite/ discrete element algorithm is developed to solve delamination interaction between different layers of composites. In the following, after a general review on the discrete element method, delamination interaction will be described in more detail, and a softening model will be introduced to simulate the crack propagation phenomena. The ability of the model to correctly simulate this behaviour will be assessed by solving two tests available in the literature.

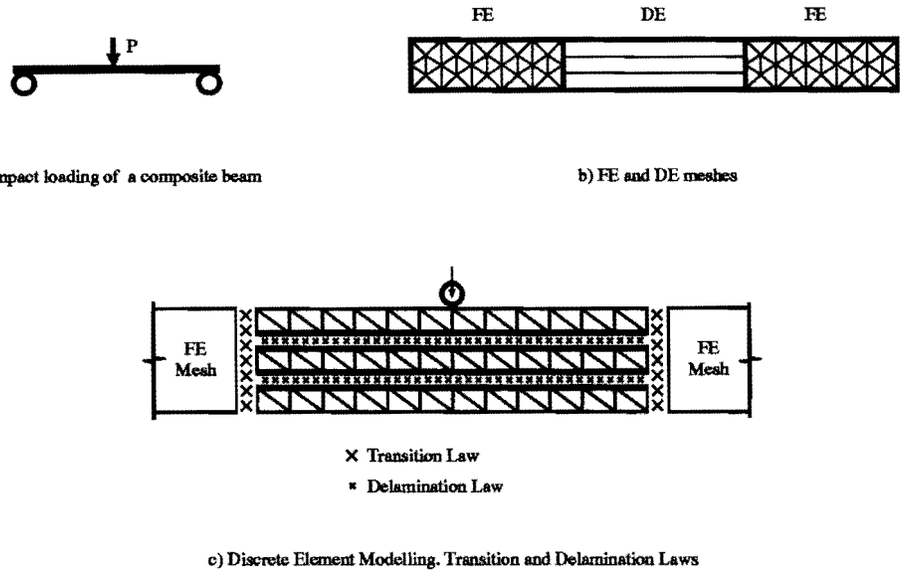

a) Impact loading of a composite beam

b) FE and DE meshes

c) Discrete Element Modelling. Transition and Delamination Laws

Figure 1: Composite beam subjected to impact loading, finite element and discrete element modelling.

2 DISCRETE ELEMENT MODELLING OF COMPOSITES

In this section a brief review of the discrete element method is presented, which will provide some particular aspects of the modelling of composites.

A typical composite beam subjected to an impact loading is shown in Figure 1a. The possible delaminated area is modelled using a discrete element mesh (Figure 1c) and the rest of the beam is modelled by a standard finite element mesh (Figure 1b). A combined mesh enables us to prevent unnecessary contact detection and interaction calculations which comprise a major part of the analysis time. It is worth noting that even by modelling the whole structure with discrete elements, we are still using a combined finite/discrete element approach, owing to the fact that finite elements are used for modelling the deformable behaviour of individual discrete elements.

Each ply or a group of similar plies is modelled by one discrete element. Each discrete element will be discretized by a finite element mesh and might have material or geometric nonlinearities. The interlaminar behaviour of discrete elements is governed by bonding laws, including contact and friction interactions for the post delamination phase. Interactions between finite elements and discrete elements are modelled by transition interfaces which prevent debonding under all stress conditions.

All interfaces, firstly, are monitored against the delamination criterion. Once two layers are delaminated, the corresponding interface will still be capable of further contact and friction interaction.

3 CONTACT INTERACTION

Once the possibility of contact between discrete elements is detected (by a contact detection algorithm), contact forces have to be evaluated to define the subsequent motion of the discrete elements from the

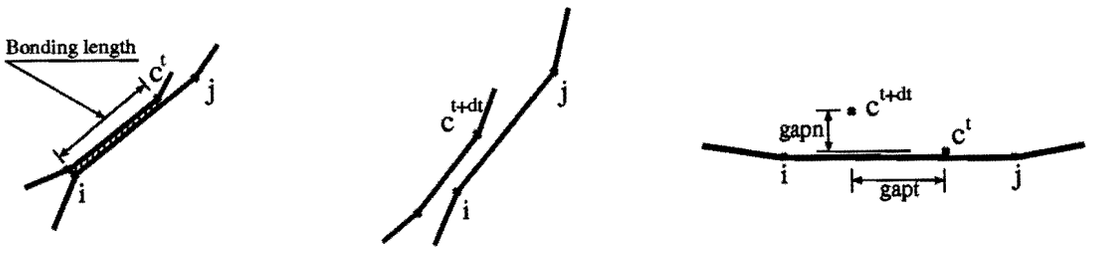

a) Bonded layers at time t

b) Debonded layers at time d+dt

c) Projection on a reference system

Figure 2: Normal and tangential gaps.

dynamic equilibrium equation.

3.1 Contact forces

According to the spatial version of the classical weak form of the boundary value problem, the component form of the virtual work of the contact forces associated to the contact node is given by [7, 8]:

$$W^c = f_k^c \, \delta \mathrm{g}_k = f_k^c \frac{\partial \mathrm{g}_k}{\partial u_i^s} \delta u_i^s \qquad (1)$$

where $k = n, t$ and $i = x, y$, and u_i^s is the the i-component of displacement vector at node s, $\mathbf{g} = (\mathrm{g}_n, \mathrm{g}_t)$ is the relative motion (gap) vector, and $\mathbf{f}^c$ is the contact force vector over the contact area A^c,

$$\mathbf{f}^c = A^c \boldsymbol{\sigma}^c \qquad (2)$$

$$\boldsymbol{\sigma}^c = \boldsymbol{\alpha}\, \mathbf{g} = \begin{bmatrix} \alpha_n & 0 \\ 0 & \alpha_t \end{bmatrix} \begin{bmatrix} \mathrm{g}_n \\ \mathrm{g}_t \end{bmatrix} \qquad (3)$$

where $\boldsymbol{\alpha}$ is the penalty term matrix, which may vary between single contact nodes. The corresponding recovered residual force is then evaluated as:

$$r_i^s = f_k^c \frac{\partial \mathrm{g}_k}{\partial u_i^s} \qquad (4)$$

The possible normal and tangential gaps for each contacting couple are evaluated by monitoring the coordinates of contacting couple nodes in each time step (Figure 2).

The calculated contact force has to be distributed to the target and the contactor nodes.

3.2 Friction law

The simple Coulomb friction law is employed to calculate friction forces. According to this assumption, there is no relative motion until the maximum allowable tangential friction force is reached,

$$\begin{array}{ll} \Delta u_t = 0 & if \quad |f_t| < \mu f_n \\ \Delta u_t \neq 0 & if \quad |f_t| = \mu f_n \end{array} \qquad (5)$$

where Δu_t is the relative tangential displacement of the two surfaces and μ is the friction coefficient.

4 DELAMINATION INITIATION

Among the several criteria that are used in prediction of the initiation of delamination in composite structures [4, 5], reasonable results can be achieved by employing the Chang-Springer criterion. Two dimensional representation of this criterion in local axes is defined by [5]:

$$\left(\frac{\sigma_{yy}}{Y^2}\right)^2 + \left(\frac{\sigma_{xy}}{S^2}\right)^2 = d^2, \begin{cases} d < 1 & \text{no failure} \\ d \geq 1 & \text{failure} \end{cases} \qquad (6)$$

where Y and S are the unidirectional normal and tangential strengths of the bonding material, respectively.

5 CRACK PROPAGATION

Within a standard central difference explicit scheme in dynamic analysis of composites, in each time step, a possible configuration is predicted from the dynamic equilibrium equations, which are formed by considering the internal forces calculated from contact/delamination interactions in the previous timestep. Therefore the current configuration offers a possible crack propagation layout which has to be modified by the new interactions in current timestep.

Once the delamination initiation criterion is satisfied, an interlaminar crack is formed, which is followed by releasing energy and redistributing the forces. To avoid mesh dependency and inaccuracy of the results [7], a local bilinear Rankine softening plasticity model is adopted.

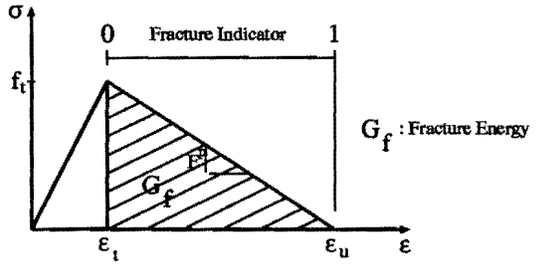

Figure 3: Rankine softening model.

The main concept is the assumption that the fracture energy release $\mathbf{G}_f$, is a material property rather than a local stress-strain curve, and is defined as the integral of the area under the softening branch of the stress-strain curve

$$G_f = \left[\frac{1}{2} f_t (\epsilon_u - \epsilon_t)\right] l_c \qquad (7)$$

where f_t is the tensile strength and ϵ_u and ϵ_t are the tensile fracture and ultimate strains respectively, and l_c is the localisation bandwidth, which is contained within one element and can be defined based on the area of the fractured element [9].

The softening modulus is then defined as

$$E^p = \frac{f_t^2 \, l_c}{2G_f} \qquad (8)$$

The position of the stress point on the softening branch, or the value of the fracture indicator (figure 3), could be used as a measure to indicate the rate of material damage in the region.

6 NUMERICAL RESULTS

In this section, two test cases are considered. Firstly, a composite bend specimen is simulated to demonstrate the capability of the method for modelling arbitrary interlaminar boundaries. In the second test case, a composite beam subjected to impact loading is modelled and it's local delamination buckling modes are numerically calculated. These results are compared with available results from the literature.

6.1 Composite bend test

Two composite bends with different angles and laminate layouts are considered. Geometric descriptions of the bend are depicted in Figure 4 and the material properties are listed in Table 1 [5]. The assumed aspect ratios are $L/H = 4$, $R/H = 4$, and $W/H = 1$.

The effects of bend angle α, ply orientation, and loading direction on delamination strength of the bend are investigated in this study.

The results of calculations by Chang and Springer [5], are listed in Table 2. These strengths were calculated the first

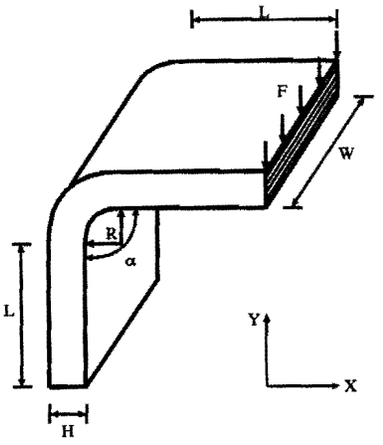

Figure 4: Geometric description of a composite bend.

$E_{xx} = 146800Mpa$	,	$G_{xx} = 6184Mpa$	
$E_{yy} = 11400Mpa$	,	$G_{yz} = 4380Mpa$	
$\nu_{xy} = \nu_{yz} = 0.3$	,	$\rho = 1.55\frac{Mg}{m^3}$	
$X_t = 1730Mpa$	,	$X_c = 1380Mpa$	
$Y_t = 66.5Mpa$	,	$Y_c = 26.8Mpa$	
$S = 133.7Mpa$			

Table 1: Material properties for T300 /1034-C graphite epoxy

R/H	$\alpha = 90$		$\alpha = 120$	
	In	Out	In	Out
1	$40(I^a)$	$17(D^b)$	$38(I)$	$15(D)$
2	–	$23(D)$	–	$24(D)$
4	–	$37(D)$	–	$37(D)$

[a] I=Inplane failure
[b] D=Delamination

Table 2: Results of $F/(W\,H)$ $[L/H = 4]$

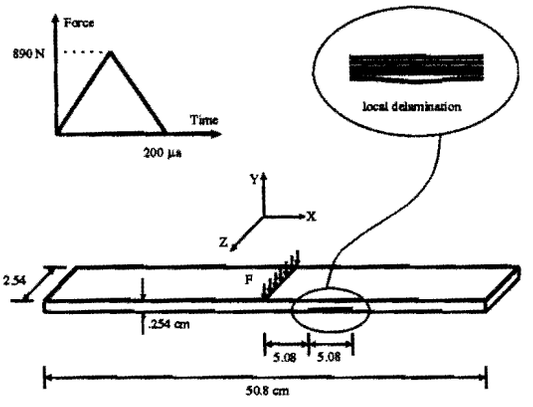

Figure 6: Specimen geometry and impact loading of a composite beam.

time that a delamination or in-plane failure occured. They concluded that for outward loadings, the failure was always caused by delamination, whereas for inward loadings, inplane fractures were the major causes of failure.

Eight and nine layer finite/discrete element models were implemented to model 90 and 120 degree bends with uniform $[0_n]$ and $[0_n/90_n/0_n]$ ply layouts, respectively. For outward loading, delamination commenced from the loaded edge of the bend and extended across the thickness and toward the clamped edge of the bend (Figures 5a,e). Analysis of results shows that for outward loadings the failure of the bend is always caused by delamination. No delamination, even in free edges is observed for inward loadings.

6.2 Buckling analysis of a composite beam

An implicit approach combined with a fracture mechanics algorithm was used by Grady *et al* [10], to perform a dynamic delamination buckling analysis in a composite laminate with an initial interlayer crack subjected to impact loading. The specimen geometry and impact loading are defined in Figure 6. The material properties of this clamped unidirectional $[0_n]$ laminate are assumed to be the same as Table

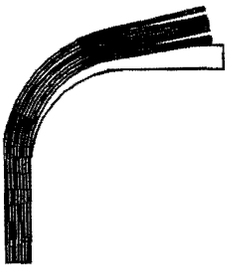

(a) Outward loading.

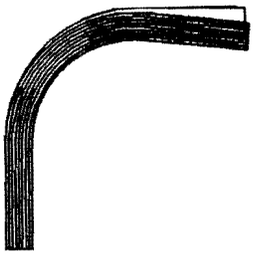

(b) Inward loading.

(c) Delamination layout.

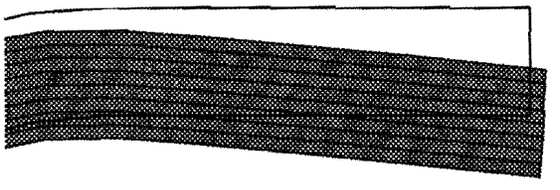

(d) No free edge delamination

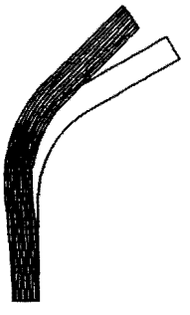

(e) Outward loading.

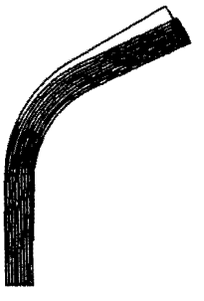

(f) Inward loading

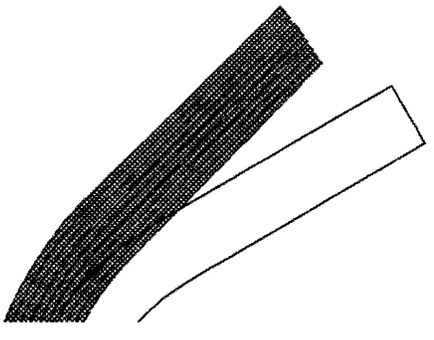

(g) Delamination layout.

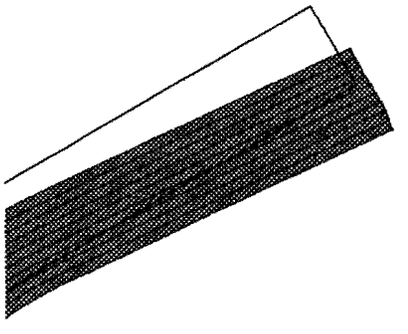

(h) No free edge delamination.

Figure 5: Deformed shapes and delamination layouts of bends. a-d)90-degree bend, e-h)120-degree bend.

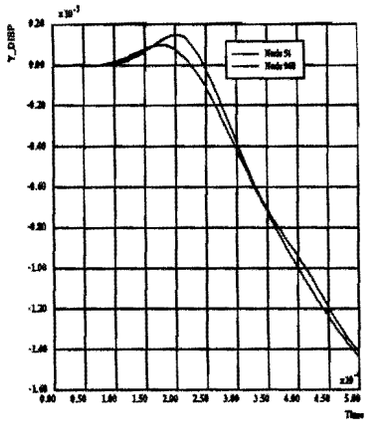

(a) Vertical displacements.

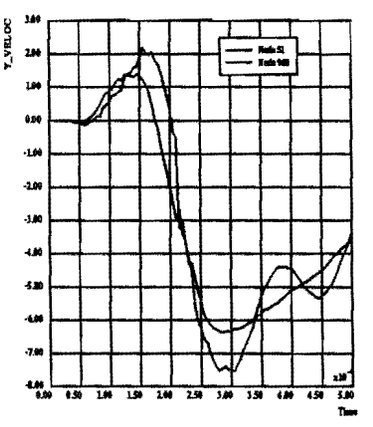

(b) Vertical velocities.

Figure 7: Time history responses of two nodes on opposite sides of the middle of initial crack.

1. They predicted that a first mode of delamination buckling is likely to occur approximately 190 μs after the impact event begins.

Four layers of discrete elements were used through the thickness to model this problem. The lowest layer is predicted to behave as a local delamination buckling. The critical timestep which ensures the stability of the scheme is restricted to $0.01\mu sec.$

The results of linear uncracked analysis and a full delamination analysis for the midpoint vertical displacements, are compared in Figure 8. It is easily concluded that the global behaviours of the beam in both cases are similar, and that the local delamination buckling does not largely effect the global response of the beam.

Figure 7 shows the time history results of vertical displacement and velocities of two adjacent nodes at the middle of the initial crack. According to Figure 7a, delamination in the middle of the crack starts at about $t = 150\mu s$ and increases rapidly after $t = 175\mu s$, therefore the possible local buckling is predicted to occur between $t = 175\mu s$ to $t = 200\mu s$. The same results may be concluded from the comparison of velocities in Figure 7b.

7 CONCLUSIONS

A combined finite / discrete element method has been successfully developed for modelling delamination behaviour of composites. The strength reduction, occuring after initiation of a crack has been considered by using a softening model. Two tests, including a composite bend and a more complex buckling analysis were used to assess the performance of the method. This method could easily be combined with an inplane fracturing algorithm to perform a full fracturing analysis of composites subjected to impact loads.

ACKNOWLEDGEMENTS

The first author would like to acknowledge the support received from the Ministry of Higher Education of I.R. IRAN.

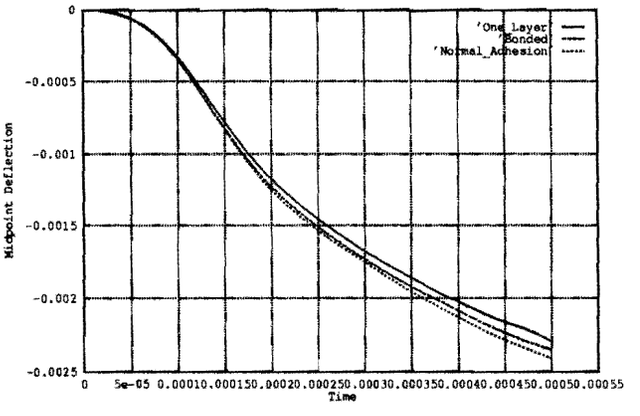

Figure 8: Midpoint Displacement

References

[1] S. Abrate. Impact resistance of composite materials - a review. *Applied Mechanics*, 44:155–190, 1991.

[2] A.J. Kinloch, Y. Wang, J.G. Williams, and P. Yayla. The mixed-mode delamination of fiber composite materials. *Composite Science and Technology*, 47:225–237, 1993.

[3] F.L. Matthews and R.D. Rawlings. *Composite Materials : Engineering and Science.* Chapman and Hall, 1994.

[4] S. Liu, Z.Kutlu, and F.K.Chang. Matrix cracking-induced delamination propagation in graphite/epoxy laminated composites due to a transverse concentrated load. In N.E.Ashbangh W.W. Stinchcomb, editor, *Composite Materials : Fatigue and Fracture, ASTM STP 1156*, volume 4. ASTM, 1993.

[5] F.K. Chang and G.S. Springer. The strength of fiber reinforced composite bends. *Composite Materials*, **20**(1), January 1986.

[6] N.Bicanic, A.Munjiza, D.R.J. Owen, and N. Petrinic. From continua to discontinua - a combined finite element / discrete element modelling in civil engineering. In B.H.V. Topping, editor, *Developments in Computational Techniques for Structural Engineering.* Civil-Comp Press, 1995.

[7] S.Mohammadi, D.R.J. Owen, and D. Peric. A combined finite/discrete element algorithm for delamination analysis of composites. Submitted for publication., 1996.

[8] M. Schonauer, T.Rodic, and D.R.J. Owen. Numerical modelling of thermomechanical processes related to bulk forming operations. *Journal De Physique IV*, **3**:1199–1209, November 1993. Colloque C7.

[9] A.J.L.Crook. Combined finite/ discrete element method. Lecture Notes, University of Wales Swansea, 1996.

[10] J.E.Grady, C.C.Chamis, and R.A.Aiello. Dynamic delamination buckling in composite laminates under impact loading : Computational simulation. In P.A. Lagace, editor, *Composite Materials: Fatigue and Fracture, ASTM STP 1012*, volume 2. ASTM, 1989.